3:1 magnetization plateau and suppression of ferroelectric polarization in an Ising chain multiferroic

Y. J. Jo,[1] Seongsu Lee,[2] E. S. Choi,[1] H. T. Yi,[2] W. Ratcliff II,[3] Y. J. Choi,[2] V. Kiryukhin,[2] S. W. Cheong,[2] and L. Balicas[1]
[1]*National High Magnetic Field Laboratory, Florida State University, Tallahassee, Florida 32310, USA*
[2]*Department of Physics and Astronomy and Rutgers Center of Emergent Materials, Rutgers University, Piscataway, New Jersey 08854, USA*
[3]*NIST Center for Neutron Research, National Institute of Standards and Technology, Gaithersburg, Maryland 20899, USA*
(Received 25 October 2008; revised manuscript received 12 December 2008; published 26 January 2009)

Ferroelectric Ising chain magnet $Ca_3Co_{2-x}Mn_xO_6$ ($x \approx 0.96$) was studied in magnetic fields of up to 33 T. Magnetization and neutron-scattering measurements reveal successive metamagnetic transitions from the zero-field $\uparrow\uparrow\downarrow\downarrow$ spin configuration to the $\uparrow\uparrow\uparrow\downarrow$ state with a broad magnetization plateau, and then to the $\uparrow\uparrow\uparrow\uparrow$ state. The absence of hysteresis in these plateaus reveals an intriguing coupling between the intrachain state and the three-dimensional geometrically frustrated magnetic system. Inversion symmetry, broken in the $\uparrow\uparrow\downarrow\downarrow$ state, is restored in the $\uparrow\uparrow\uparrow\downarrow$ state, leading to the complete suppression of the electric polarization driven by symmetric superexchange.

DOI: 10.1103/PhysRevB.79.012407 PACS number(s): 75.25.+z, 71.18.+y, 71.30.+h, 72.15.Gd

Recent discoveries of new multiferroics (compounds exhibiting both magnetism and ferroelectricity) that display a coupling between the corresponding order parameters have triggered a resurgence in the field of the magnetoelectric effect.[1–4] In many of these materials, magnetic order breaks inversion symmetry, and electric polarization is subsequently induced via magnetoelastic coupling. Typically, such magnetism-driven ferroelectricity is found in spiral magnets, in which the spin-lattice coupling arises due to the Dzyaloshinskii-Moriya interaction, which is associated with the antisymmetric part of the exchange coupling.[1] This mechanism is realized in $TbMnO_3$, $Ni_3V_2O_8$, $CuFeO_2$, and many other systems.[1,5–7] However, because of the weakness of the antisymmetric exchange, the induced electric polarization in these systems is rather small. Exchange striction associated with symmetric superexchange coupling is, in general, a considerably larger effect. It may give rise to giant atomic displacements, such as those recently observed in hexagonal $(YLu)MnO_3$,[8] and thereby affect dielectric properties. Multiferroics with symmetric exchange striction therefore hold significant promise as candidate materials for giant magnetoelectric effects.

A remarkable example of the latter system is a recently discovered multiferroic Ising chain magnet $Ca_3Co_{2-x}Mn_xO_6$ (for $x \approx 0.96$).[9] It is composed of *c*-axis spin chains consisting of magnetic ions within alternating oxygen cages of face-shared trigonal prisms and octahedra. The spin chains are separated by the Ca ions and form a triangular lattice within the *ab* plane. For $x=1$, all Co ions are located in the prismatic sites, while all the Mn ions occupy the octahedral sites.[10] Because of the frustrated ferromagnetic nearest-neighbor (nn) and antiferromagnetic next-nearest-neighbor (nnn) interactions within the chains, an $\uparrow\uparrow\downarrow\downarrow$ magnetic order forms for $T < T_c \approx 16$ K.[9] Combined with the alternating Co^{2+} and Mn^{4+} ionic order, this breaks the inversion symmetry and induces an electric polarization along the chain via symmetric magnetostriction.[1,9] Thus, this system combines physics of frustrated Ising chain with physics of magnetically driven ferroelectricity. Frustrated Ising chains were extensively studied theoretically,[11,12] but good experimental realizations were proven hard to find. In addition, because of the triangular coordination of the chains within the *ab* plane, the interchain interaction is geometrically frustrated. Effects of frustration are revealed in this material by the observation of a magnetic freezing transition at $T_F \approx 3$ K.[9] Here we explore the effects of the application of an external magnetic field on the magnetic and ferroelectric response of $Ca_3Co_{2-x}Mn_xO_6$ (for $x \approx 0.96$). This is of great interest given the complex interplay between the physics of frustrated Ising spin chains, the magnetoelectric effect, and the geometrically frustrated magnetism. Below, we show that $Ca_3Co_{2-x}Mn_xO_6$ provides a remarkable model in which to explore the interrelation among these phenomena.

Single crystals of $Ca_3Co_{1.04}Mn_{0.96}O_6$ were grown by the flux method described in Ref. 9, producing needlelike single crystals. These were cut in a convenient geometry for dielectric constant ε and electric polarization P measurements, with a cross-sectional area of 0.45–0.55 mm^2 and thickness of 0.32–0.35 mm. To remove any strain left by the cutting and polishing procedure, the crystals were annealed at 650 °C for 5 h. Two electrodes were painted onto the largest surfaces of the crystals. ε was obtained by measuring the capacitance as a function of temperature or field with a manual capacitance bridge, using an excitation signal of 30 V at 5 kHz. To obtain the temperature and the magnetic field dependence of the electric polarization P, the pyroelectric and magnetoelectric currents were measured with an electrometer at rates of, respectively, 3 K/min and 5 T/min, after cooling the specimens from 40 to 1.5 K in a static poling electric field $E_{pole}=5.63$ kV/m. $P(T,H)$ was measured after removing the poling field. Magnetization measurements were performed by using a vibrating sample magnetometer in magnetic fields of up to 33 T coupled to a ^{3}He refrigerator provided by the NHMFL. Neutron powder-diffraction measurements were performed in polycrystalline samples of $Ca_3Co_{1.05}Mn_{0.95}O_6$ at the BT-7 beamline at the NIST Center for Neutron Research. The specimen was loaded in an 11 T vertical field magnet. The data were collected at $T=1.6$ K in

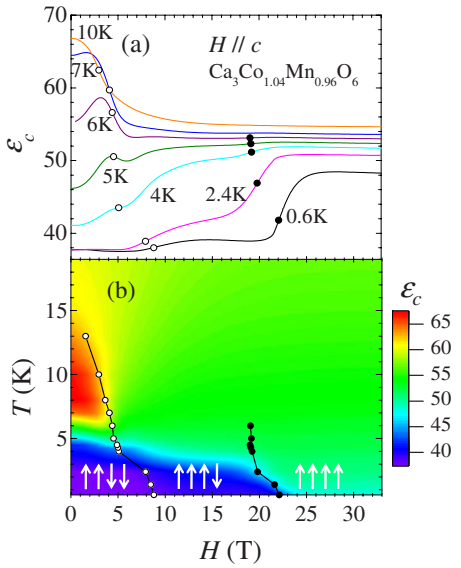

FIG. 1. (Color online) (a) Dielectric constant ε_c for a $Ca_3Co_{1.04}Mn_{0.96}O_6$ single crystal for an electric field applied along the c axis and as a function of the magnetic field H applied in the same direction. (b) Contour plot displaying the behavior of ε_c in the T-H plane. Circles indicate magnetic transitions. Spin configurations are shown with arrows (see text). Open and closed circles correspond in both figures to the maximums in the derivative of ε_c respect to the field which are associated with the field-induced phase transitions.

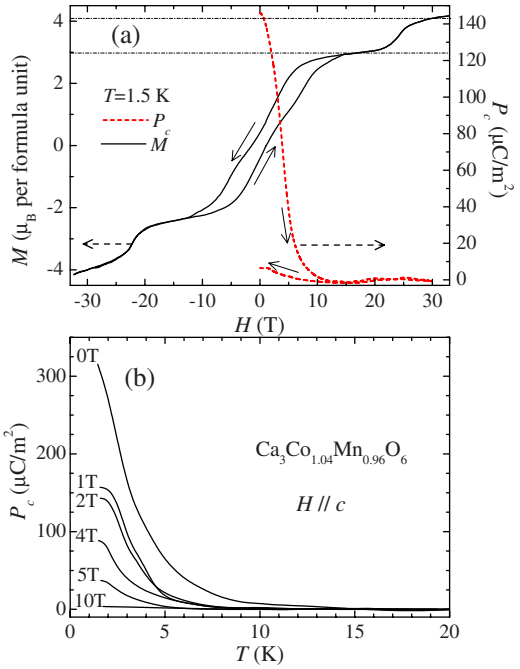

FIG. 2. (Color online) (a) Magnetization M and c-axis electric polarization P_c as functions of the field H applied along the c axis at $T=1.5$ and 1.4 K, respectively. Notice the marked hysteresis on both M and P_c among field up and down sweeps. (b) Electric polarization P_c as a function of temperature for several values of c-axis magnetic field.

the horizontal scattering plane by using monochromatic neutrons with wavelength of 2.3592 Å. The diffraction data were refined using the FULLPROF program package.[13] Due to strong magnetocrystalline anisotropy, the crystallites tend to orient along the c axis in applied magnetic fields. A correction for this effect (preferred orientation), obtained from refinement of the nuclear structure only, was applied in the final refinement of the magnetic and nuclear structures.

Figure 1(a) shows the magnetic field dependence of the dielectric constant ε_c for an electric field along the chain direction, i.e., $E\|c$, and for several temperatures. The magnetic field was also applied along the chain direction. As seen, ε_c displays broad temperature-dependent features: a broad peak below 5 T that is displaced to higher fields as T is decreased, and a step for $20 \leq H \leq 25$ T. As shown below, both features coincide with field-induced magnetic and ferroelectric transitions. The overall dependence of ε_c on H and T is displayed in Fig. 1(b), which shows a contour plot of ε_c in the T-H plane. ε_c shows a broad maximum around ~ 10 K, which is several degrees below the magnetic phase transition to the $\uparrow\uparrow\downarrow\downarrow$ spin state, with all the spins pointing along the c axis.[9] The discrepancy between the temperatures of the magnetic transition and the maximum in ε_c results from the freezing effects and corresponding quasi-long-range magnetic order.[9] As shown in Ref. 9 these effects also cause the magnetoelectric freezing transition for $T < 5$ K, which is revealed in the behavior of the magnetic susceptibility, as well as in the marked suppression of ε_c clearly observed in the data of Fig. 1(b).

To elucidate the origin of the features observed in ε_c, we performed magnetization (M) measurements as a function of magnetic field applied along the chain direction. A representative curve is shown in Fig. 2(a) for $T=1.5$ K. Two major features are observed in $M(H)$, largely coinciding with the structures seen in ε_c. The first feature at approximately 10 T leads to a very broad plateau at a value of $\sim 3\mu_B$, corresponding to the full saturation moment of Mn^{4+}, thus indicating that the Mn sublattice becomes ferromagnetic above this field. A second quasiplateau is observed above 25 T with a saturation moment of $\sim 4\mu_B$, corresponding to a fully polarized spin state of high-spin Mn^{4+} and low-spin Co^{2+} moments with no apparent large orbital contribution found in neutron-diffraction experiments.[9] Thus M indicates that the $\uparrow\uparrow\uparrow\downarrow$ spin state with *all* Mn^{4+} moments aligned along the field is stabilized for $10 \leq H \leq 25$ T, and that the system becomes ferromagnetic at higher fields. Importantly, this sequence of transitions is predicted by the alternating-spin Ising ferrimagnet model with competing nn and nnn interactions in a large parameter range.[12] It is therefore probable that such a simple model is physically realized in our system. Finally, in our single crystals, geometrical frustration leads to magnetic domain formation at $H=0$.[9] This would explain the hysteretic behavior seen in M for $0 \leq H \leq 15$ T. Intriguingly, it disappears once the $\uparrow\uparrow\uparrow\downarrow$ state is stabilized. The absence of hysteresis in the plateau region suggests that the interchain geometric frustration has somehow been lifted. Therefore, a transition in the one-dimensional (1D) magnetic subsystem seems to relieve the geometrical frustration in the three-dimensional (3D) lattice, an aspect that clearly deserves theoretical attention.

Measurements of the electrical polarization P_c as a func-

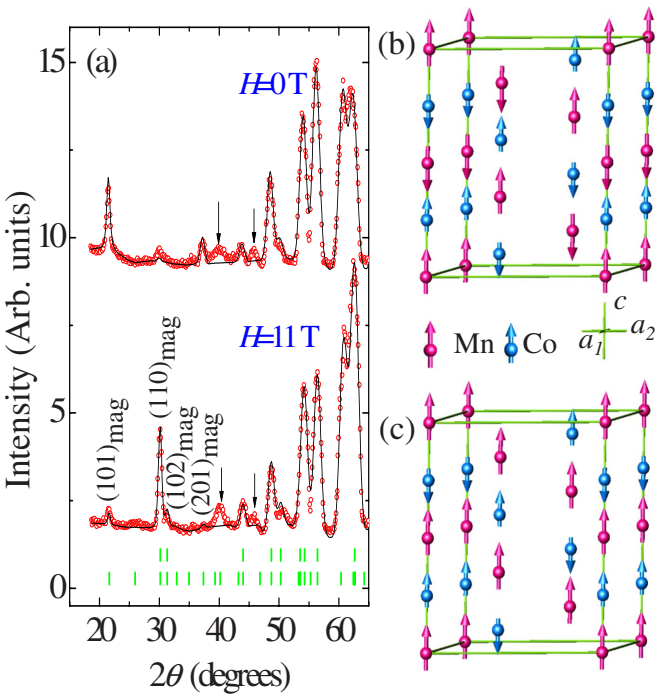

FIG. 3. (Color online) (a) Observed (symbols) and calculated (line) powder neutron-diffraction patterns for $H=0$ and 11 T, both at $T=1.6$ K. The bars below the patterns indicate positions for nuclear (first row) and magnetic (second row) Bragg peaks. Arrows show the impurity phase. (b) Zero-field magnetic $\uparrow\uparrow\downarrow\downarrow$ structure (Ref. 9). (c) The $\uparrow\uparrow\uparrow\downarrow$ magnetic structure obtained in the refinement of the 11 T data. Mn ions are represented by longer arrows while shorter ones represent Co ions.

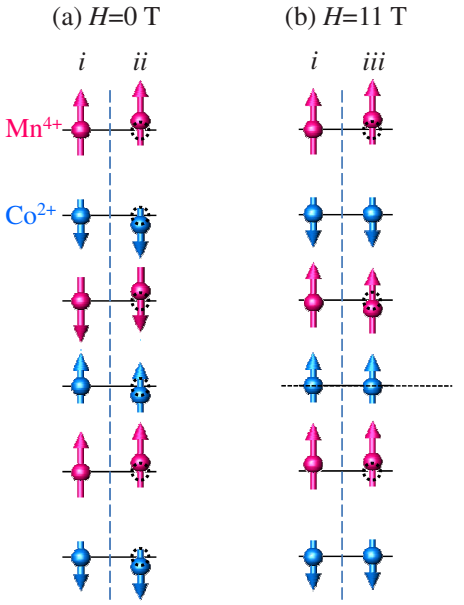

FIG. 4. (Color online) (a) A sketch representing the Ising chains with the zero-field $\uparrow\uparrow\downarrow\downarrow$ spin order and alternating ionic charge order, in which electric polarization is induced through symmetric exchange striction. The corresponding displacements of the Mn (longer arrows) and Co (shorter arrows) ions along the spin chain are depicted in (ii) relative to their positions (i) in a uniform chain. (b) The $\uparrow\uparrow\uparrow\downarrow$ plateau state without (i) and with (ii) the ionic displacements due to the exchange striction. This magnetic and charge order possesses an inversion symmetry center (horizontal line).

tion of both temperature and magnetic field applied along the chain direction reveal a giant magnetoelectric effect. In Fig. 2(a) we show the electrical polarization P_c as a function of H at a temperature $T=1.4$ K. Application of an external field quickly suppresses $P_c(T)$, which disappears completely for fields exceeding ~ 10 T, i.e., as the $\uparrow\uparrow\uparrow\downarrow$ plateau is stabilized in M. Figure 2(b) shows the temperature dependence of P_c for several values of the external field indicated in the figure. In agreement with the previous report,[9] at zero field and below 15 K, P_c gradually increases reaching a value of 310 μC/m^2 at 2 K. The polarization is completely suppressed above the magnetic transition fields determined from the M and ε_c curves shown in Figs. 1 and 2. Thus, our data show that the field-induced transition from the $\uparrow\uparrow\downarrow\downarrow$ to the $\uparrow\uparrow\uparrow\downarrow$ structure leads to the total suppression of the electric polarization. We note that the observed strong magnetoelastic coupling may play a role in the stabilization of the broad $\uparrow\uparrow\uparrow\downarrow$ plateau, as it does in the case of a similar 3:1 plateau observed in MCr_2O_4 spinels.[14]

To confirm the spin structure suggested by the magnetization measurements, we performed neutron powder-diffraction measurements. Figure 3 shows the obtained data at $T=1.6$ K for fields of zero and 11 T. The zero-field data confirm the $\uparrow\uparrow\downarrow\downarrow$ structure reported in Ref. 9. In a polycrystalline sample, the crystallites exhibit all possible orientations with respect to the external field, and therefore for some of them the c-axis projection of the field is always smaller than the critical field needed to stabilize the $\uparrow\uparrow\uparrow\downarrow$ state. The critical field may also depend on location in the multidomain magnetic state. Thus, in an applied magnetic field of 11 T, the sample is expected to contain a mixture of both the $\uparrow\uparrow\downarrow\downarrow$ and $\uparrow\uparrow\uparrow\downarrow$ states, with each domain exhibiting its own spin canting angle with respect to the c axis. The canting angle averages to zero over the entire sample. The 11 T magnetic structure was refined assuming the presence of both of the structures with no spin canting. The resulting fit ($R_B=5.7\%$, $R_M=12.8\%$) is shown in Fig. 3. The Mn^{4+} moments are $2.20(7)\mu_B$ and are ordered ferromagnetically, while the Co^{2+} are ordered antiferromagnetically with a moment of $0.75(8)\mu_B$, as shown in Fig. 3(c). The obtained volume fractions for the $\uparrow\uparrow\downarrow\downarrow$ and $\uparrow\uparrow\uparrow\downarrow$ phases at 11 T are 10% and 90%, respectively. We note that at 11 T, most of the grains have their c axis oriented along the field, and therefore the c-axis field component is large enough to stabilize the $\uparrow\uparrow\uparrow\downarrow$ state in the majority of the grains. This state is therefore obtained even in a single-phase refinement, albeit with a small (unphysical) canting angle. Thus, in agreement with the magnetization data, neutron diffraction also shows that the $\uparrow\uparrow\uparrow\downarrow$ state is realized at 11 T. The complete suppression of the electric polarization on the transition to the $\uparrow\uparrow\uparrow\downarrow$ state can be easily explained on symmetry grounds. Figure 4 shows the (a) $\uparrow\uparrow\downarrow\downarrow$ and (b) $\uparrow\uparrow\uparrow\downarrow$ undistorted chains (i), and the same chains but with ionic displacements expected as a result of exchange striction (ii and iii). Due to the ionic order in the chains, collinear electric dipoles form in (ii).[9] In contrast, as shown in Fig. 4(b), the $\uparrow\uparrow\uparrow\downarrow$ state possesses inver-

sion symmetry, and therefore (iii) should lack the polarization, in agreement with our measurements.

It is well known that interactions between the chains on a frustrated triangular lattice play a major role in the parent compound of our series, $Ca_3Co_2O_6$.[15] Unlike in our compound, the chains in $Ca_3Co_2O_6$ are ferromagnetic and lack intrachain degrees of freedom. Hysteretic magnetization plateaus are also observed in this compound, but they are associated with the interchain magnetic order.[16,17] In contrast, the major features of $Ca_3Co_{2-x}Mn_xO_6$ as discussed above are dominated by the physics of a single Ising chain. However, some of our data are likely to require explanations going beyond this simple model. A significant hysteresis is observed until the $\uparrow\uparrow\uparrow\downarrow$ plateau is achieved (Fig. 2), and a freezing transition occurs at low temperatures (Fig. 1 and Ref. 9). Frustrated interchain interactions are expected to play a role for all these effects. The zero-field state is known to lack true long-range order and to contain finite-size magnetoelectric domains, probably due to both the frustrated interchain interactions and the one dimensionality of this system.[9] Gradual magnetization changes, as well as hysteresis, are expected when a magnetic field is applied and the domains are gradually converted into the $\uparrow\uparrow\uparrow\downarrow$ state. The gradual decrease in P_c in an applied field is probably also associated with these effects. A sharper magnetization feature may be expected at the transition from the well-ordered $\uparrow\uparrow\uparrow\downarrow$ state to the $\uparrow\uparrow\uparrow\uparrow$ state in this Ising system, as is indeed seen in the data of Fig. 2(a). These effects are interesting and clearly deserve further investigation. Thus, while the major features of the phase diagram of $Ca_3Co_{1.05}Mn_{0.95}O_6$ are established in our work, further work on this material should be of interest in the context of the physics of frustrated chain magnets, geometrical frustration, and magnetically driven ferroelectricity.

In conclusion, $Ca_3Co_{2-x}Mn_xO_6$ ($x \simeq 0.96$) provides a unique experimental realization of a system of internally frustrated Ising chains assembled on a geometrically frustrated triangular lattice. Magnetic field induces a transition from the zero-field $\uparrow\uparrow\downarrow\downarrow$ state characterized by glassiness, to the $\uparrow\uparrow\uparrow\downarrow$ spin-solid state, and then to the fully ferromagnetic state. The $\uparrow\uparrow\uparrow\downarrow$ configuration is associated with a magnetization plateau that does not display any magnetic hysteresis, indicating that this compound displays a unique interplay between the intrachain magnetism and the geometric frustration inherent to its three-dimensional triangular lattice. This aspect has yet to be considered theoretically. We find that a remarkably simple magnetoelectric model system is realized in this compound. While the $\uparrow\uparrow\downarrow\downarrow$ state is ferroelectric due to exchange striction, the field-induced $\uparrow\uparrow\uparrow\downarrow$ state should possess inversion symmetry. Consistently, we find that electric polarization is destroyed in the latter state, giving rise to the observed giant magnetoelectric effect.

The NHMFL is supported by NSF through Grant No. NSF-DMR-0084173 and the State of Florida. L.B. acknowledges the NHMFL in-house research program and Y.J.J. acknowledges the NHMFL-Schuller program. Work at Rutgers was supported by the DOE under Grant No. DE-FG02-07ER46382. S.L. was partially supported by the Korea Science and Engineering Foundation through the Center for Strongly Correlated Materials Research at Seoul National University.

[1] S.-W. Cheong and M. Mostovoy, Nature Mater. **6**, 13 (2007).
[2] M. Fiebig, J. Phys. D **38**, R123 (2005).
[3] D. I. Khomskii, J. Magn. Magn. Mater. **306**, 1 (2006).
[4] W. Eerenstein, N. D. Mathur, and J. F. Scott, Nature (London) **442**, 759 (2006).
[5] T. Kimura, T. Goto, H. Shintani, K. Ishizaka, T. Arima, and Y. Tokura, Nature (London) **426**, 55 (2003).
[6] G. Lawes, A. B. Harris, T. Kimura, N. Rogado, R. J. Cava, A. Aharony, O. Entin-Wohlman, T. Yildrim, M. Kenzelmann, C. Broholm, and A. P. Ramirez, Phys. Rev. Lett. **95**, 087205 (2005).
[7] T. Kimura, J. C. Lashley, and A. P. Ramirez, Phys. Rev. B **73**, 220401(R) (2006).
[8] S. Lee, A. Pirogov, M. S. Kang, K. H. Jang, M. Yonemura, T. Kamiyama, S. W. Cheong, F. Gozzo, N. Shin, H. Kimura, Y. Noda, and J. G. Park, Nature (London) **451**, 805 (2008).
[9] Y. J. Choi, H. T. Yi, S. Lee, Q. Huang, V. Kiryukhin, and S. W. Cheong, Phys. Rev. Lett. **100**, 047601 (2008).
[10] V. G. Zubkov, G. V. Bazuev, A. P. Tyutyunnik, and I. F. Berger, J. Solid State Chem. **160**, 293 (2001).
[11] W. Selke, Phys. Rep. **170**, 213 (1988).
[12] J.-J. Kim, S. Mori, and I. Harada, J. Phys. Soc. Jpn. **65**, 2624 (1996).
[13] J. Rodríguez-Carvajal, Physica B **192**, 55 (1993).
[14] H. Ueda, H. A. Katori, H. Mitamura, T. Goto, and H. Takagi, Phys. Rev. Lett. **94**, 047202 (2005); H. Ueda, H. Mitamura, T. Goto, and Y. Ueda, Phys. Rev. B **73**, 094415 (2006).
[15] S. Aasland, H. Fjellvag, and B. Hauback, Solid State Commun. **101**, 187 (1997).
[16] V. Hardy, M. R. Lees, O. A. Petrenko, D. McK. Paul, D. Flahaut, S. Hébert, and A. Maignan, Phys. Rev. B **70**, 064424 (2004).
[17] V. Hardy, D. Flahaut, M. R. Lees, and O. A. Petrenko, Phys. Rev. B **70**, 214439 (2004).